Journal of Translational Medicine

RESEARCH

Open Access

Nilotinib boosts the efficacy of anti-PDL1 therapy in colorectal cancer by restoring the expression of MHC-I

Haiyan Dong[1,2,5,6,7†], Chuangyu Wen[3,4*†], Lu He[2,5,6,7,8], Jingdan Zhang[1,2,5,6,7], Nanlin Xiang[1,2,5,6,7], Liumei Liang[1,2,5,6,7], Limei Hu[9], Weiqian Li[1,2,5,6,7], Jiaqi Liu[1,2,5,6,7], Mengchen Shi[1,2,5,6,7], Yijia Hu[1,2,5,6,7], Siyu Chen[10], Huanliang Liu[1,2,5,6,7*] and Xiangling Yang[1,2,5,6,7*]

Abstract

Background Although immune checkpoint inhibitors (ICIs) have revolutionized the landscape of cancer treatment, only a minority of colorectal cancer (CRC) patients respond to them. Enhancing tumor immunogenicity by increasing major histocompatibility complex I (MHC-I) surface expression is a promising strategy to boost the antitumor efficacy of ICIs.

Methods Dual luciferase reporter assays were performed to find drug candidates that can increase MHC-I expression. The effect of nilotinib on MHC-I expression was verified by dual luciferase reporter assays, qRT-PCR, flow cytometry and western blotting. The biological functions of nilotinib were evaluated through a series of in vitro and in vivo experiments. Using RNA-seq analysis, immunofluorescence assays, western blotting, flow cytometry, rescue experiments and microarray chip assays, the underlying molecular mechanisms were investigated.

Results Nilotinib induces MHC-I expression in CRC cells, enhances $CD8^+$ T-cell cytotoxicity and subsequently enhances the antitumor effects of anti-PDL1 in both microsatellite instability and microsatellite stable models. Mechanistically, nilotinib promotes MHC-I mRNA expression via the cGAS-STING-NF-κB pathway and reduces MHC-I degradation by suppressing PCSK9 expression in CRC cells. PCSK9 may serve as a potential therapeutic target for CRC, with nilotinib potentially targeting PCSK9 to exert anti-CRC effects.

Conclusion This study reveals a previously unknown role of nilotinib in antitumor immunity by inducing MHC-I expression in CRC cells. Our findings suggest that combining nilotinib with anti-PDL1 therapy may be an effective strategy for the treatment of CRC.

Keywords Colorectal cancer, Nilotinib, Anti-PDL1 therapy, MHC-I, $CD8^+$ T cell

†Haiyan Dong and Chuangyu Wen were co-first authors.

*Correspondence:
Chuangyu Wen
chuangyu@uchicago.edu
Huanliang Liu
liuhuanl@mail.sysu.edu.cn
Xiangling Yang
yangxl28@mail.sysu.edu.cn
Full list of author information is available at the end of the article

Background

Immune checkpoint inhibitors (ICIs) have revolutionized the landscape of cancer treatment [1, 2]. In colorectal cancer (CRC), ICIs such as nivolumab, which target the programmed cell death protein 1 (PD-1)/programmed cell death-ligand 1 (PD-L1) axis, have been approved for treating patients with mismatch repair deficiency (dMMR) or high microsatellite instability (MSI-H), as dMMR/MSI-H patients are associated with a high mutation burden and tumor neoantigen load [3, 4]. However, only approximately 15% of CRC patients are diagnosed with dMMR/MSI-H status, more than 50% of CRC patients with dMMR/MSI-H status show resistance to ICIs [5, 6]. Therefore, there is an urgent need to explore new strategies to enhance the antitumor efficacy of ICIs.

The success of antitumor immunity relies on $CD8^+$ cytotoxic T cells, which recognize and kill tumor cells via interactions between T-cell receptors and tumor-related antigens presented on major histocompatibility complex I (MHC-I) [7–9]. MHC-I comprises a polymorphic heavy chain, which is encoded by the human leukocyte antigen (HLA)-A, HLA-B, and HLA-C genes, and an invariant β2-microglobulin (β2m) in humans [10]. MHC-I molecules are displayed on the cell surface and are required for antigen presentation [11]. In tumors with sufficient MHC-I antigen presentation, ICIs can alleviate $CD8^+$ T-cell exhaustion and enable sustained immune protection. However, ICIs are limited in their ability to trigger $CD8^+$ T-cell responses against tumor cells due to insufficient MHC-I antigen presentation, which reduces the sensitivity of tumors to ICIs [12].

The downregulation of MHC-I expression on tumor cells has been reported to occur in various cancer types, including CRC, and serves as a major immune escape mechanism of tumor cells to evade recognition and killing by $CD8^+$ T-cells [13–15]. Thus, enhancing tumor immunogenicity by increasing MHC-I surface expression is a promising strategy to enhance $CD8^+$ T-cell-mediated cytotoxic function and ICI efficacy. Increasing evidence has shown that the application of small molecule compounds for restoring MHC-I expression has great potential [16–18]. For instance, Xu et al. reported that atractylenolide I, a major bioactive component of the Chinese herbal medicine Rhizoma Atractylodes Macrocephalae, can upregulate MHC-I expression, enhance the responsiveness to PD1 blockade and exhibit a notable antitumor effect [19]. Given that the approved drugs have well-characterized biological activity, safety, and bioavailability properties, we conducted a drug screening using the FDA-approved drug library (ApexBio, L1021) to identify compounds capable of inducing MHC-I expression in CRC cells, and we found that nilotinib could significantly upregulate MHC-I expression.

Nilotinib is a second-generation tyrosine kinase inhibitor that inhibits various kinases, including Bcr-Abl, DDR, KIT and PDGFR. It has been approved by the FDA for the treatment of imatinib-resistant chronic myeloid leukemia [20, 21]. Recently, it has been reported that nilotinib directly eradicates several types of solid tumors [22–24]. However, the effect of nilotinib on the antitumor T-cell response remains unclear, and whether nilotinib can be used to promote the efficacy of ICIs in CRC treatment needs further investigation.

In this study, our results show that nilotinib significantly upregulates the expression of MHC-I, promotes antitumor $CD8^+$ T-cell activation, and increase the response of both MSI-high and MSS CRC tumors to anti-PDL1 therapy. Mechanistically, nilotinib upregulates MHC-I mRNA expression via the cGAS-STING-NF-κB pathway and inhibites MHC-I degradation by downregulating proprotein convertase subtilisin/kexin type 9 (PCSK9) expression in CRC cells. Our results pave the way for the combination of nilotinib with ICIs in the clinic to improve the effectiveness of ICIs in patients with CRC.

Methods

Cell culture and reagents

CRC cell lines (HCT116, SW480, and CT26) and the human embryo kidney cell line HEK293T were purchased from the American Type Culture Collection (ATCC). MC38 cells were acquired from the Culture Collection of the Chinese Academy of Science (Shanghai, China). MC38 and HEK293T cells were cultured in DMEM, while HCT116, SW480 and CT26 cells were cultured in RPMI 1640. Both media, sourced from Gibco Life Technologies (Carlsbad, CA, USA), were supplemented with 10% fetal bovine serum, 100 U/mL penicillin, and 10 μg/mL streptomycin (Gibco Life Technologies, Carlsbad, CA, USA). The cells were incubated at 37 ℃ in an incubator with 5% CO_2.

Nilotinib (ApexBio, TX, USA), JSH-23 (Selleck, TX, USA) and H151 (Selleck) were solubilized in DMSO and stored at − 20 °C. Primary antibodies against p65 and phospho-p65 (p-p65) were purchased from Beyotime (Jiangsu, China). Antibodies against β2m, STING, phospho-STING (p-STING) and Na-K-ATPase were purchased from Cell Signaling Technology (Danvers, MA, USA). The HLA-A antibody was purchased from Abcam (Cambridge, MA, USA). Antibodies against GAPDH, LaminB1, PCSK9, anti-rabbit immunoglobulin G, and anti-mouse immunoglobulin G horseradish peroxidase-conjugated secondary antibodies were purchased from Proteintech Group (Chicago, IL, USA).

Dual luciferase reporter assay

HCT116 and SW480 cells were transfected with the HLA-A2, β2M or NF-κB firefly luciferase reporter plasmids. The Renilla luciferase reporter plasmid was used as an internal reference. Following transfection, the cells were plated in 96-well plates and exposed to varying concentrations of nilotinib. Firefly and Renilla luciferase activities were subsequently detected using a Promega Luciferase Assay Kit (Madison, WI, USA) and quantified on a 96-well plate reader (Thermo Fisher Scientific, Waltham, MA, USA).

Quantitative real-time PCR (qRT–PCR) analysis

Total RNA was extracted using an RNA-Quick Purification Kit (Shanghai Yishan Biotechnology Co., Ltd., Shanghai, China) according to the manufacturer's instructions. For cDNA synthesis, PrimeScript RT Master Mix (TaKaRa, Dalian, Liaoning, China) was utilized. qRT-PCR was conducted with a SYBR Green Premix Ex Taq II kit (TaKaRa). The expression levels of mRNA targets were normalized to those of GAPDH, analyzed via the $2^{-\Delta\Delta CT}$ method, and presented as fold change of control. The primer sequences used are as follows:

human HLA-A forward: 5′-GGGTCCGGAGTATTG GGACGG-3′;

human HLA-A reverse: 5′-TTGCCGTCGTAGGCG TACTGGTG-3′;

human β2M forward: 5′-GAGGCTATCCAGCGT ACTCCA-3′;

human β2M reverse: 5′-CGGCAGGCATACTCA TCTTTT-3′;

human PCSK9 forward: 5′-CCTGGAGCGGATTAC CCCT-3′;

human PCSK9 reverse: 5′-CTGTATGCTGGTGTC TAGGAGA-3′;

human GAPDH forward: 5′-GCACCGTCAAGG CTGAGAAC-3′;

human GAPDH reverse: 5′-TGGTGAAGACGCCAG TGGA-3′;

human β-actin forward: 5′-AGAGCTACGAGCTGC CTGAC-3′;

human β-actin reverse: 5′-AGCACTGTGTTGGCG TACAG-3′;

mouse PCSK9 forward: 5′-TTGCCCCATGTGGAG TACATT-3′;

mouse PCSK9 reverse: 5′-GGGAGCGGTCTTCCT CTGT-3′;

mouse STING forward: 5′-TCGCACGAACTTGGA CTACTG-3′;

mouse STING reverse: 5′-CCAACTGAGGTATAT GTCAGCAG-3′;

mouse GAPDH forward: 5′-TGACCTCAACTACAT GGTCTACA-3′;

mouse GAPDH reverse: 5′-CTTCCCATTCTCGGC CTTG-3′;

Flow cytometry assay

Cell sample analysis

After various treatments, the cells were harvested and washed with PBS. The cells were then suspended in 100 μl of PBS, and specific fluorescent antibodies targeting surface markers were added, followed by a 20 min incubation at 4 °C. The following fluorescent antibodies were obtained from Biolegend (San Diego, CA, USA): FITC-conjugated anti-human HLA-A2, APC-conjugated anti-human HLA-A2, PE-conjugated anti-human β2-microglobulin, and PE-conjugated anti-mouse H-2 Kb bound to SIINFEKL.

Tissue sample analysis

Tumor tissues were digested using a combination of collagenase and DNase to obtain single-cell suspensions. PE-conjugated anti-mouse H-2 kb (BioLegend), FITC-conjugated anti-mouse H-2 kb (BioLegend) and APC-conjugated anti-mouse H-2kd (BioLegend) antibodies were used to analyze the expression of surface molecules. To determine the activation status of tumor-infiltrating $CD8^+$ T cells, the cells were treated with the Cell Activation Cocktail (with Brefeldin A) from BioLegend for 6 h at 37 °C. A Zombie NIR™ Fixable Viability Kit (BioLegend) was used for dead cell labeling. The cells were stained with FITC-conjugated anti-mouse CD45 (BioLegend), PE-conjugated anti-mouse CD8a (BioLegend) and Alexa Fluor® 700-conjugated anti-mouse CD4 (BioLegend) antibodies. For intracellular marker staining, the cells were processed using a fixation/permeabilization kit (BD Biosciences, USA) and stained with an APC-conjugated anti-mouse IFN-γ antibody (BioLegend).

Flow cytometry data were acquired on a CytoFLEX instrument (Beckman Coulter, CA, USA) and analyzed using FlowJo software.

Western blot analysis

Nuclear and cytoplasmic proteins were extracted using a Cytoplasmic and Nuclear Protein Extraction Kit (KeyGen Biotech, Nanjing, Jiangsu, China) following the manufacturer's instructions. Cell membrane proteins were isolated using a Membrane Protein Extraction Kit (KeyGen Biotech) according to the manufacturer's instructions. For total protein extraction, cells were lysed in RIPA lysis buffer (Cell Signaling Technology) supplemented with phosphatase and protease inhibitors (KeyGen Biotech).

The protein concentrations in the samples were ascertained using a BCA Protein Quantitation Kit (Thermo

Fisher Scientific). Proteins were resolved via SDS–PAGE and subsequently electroblotted onto a polyvinylidene fluoride (PVDF) membrane. After transfer, the membranes were blocked with 5% bovine serum albumin or 5% nonfat dry milk. The blocked membranes were incubated with primary antibodies overnight at 4 °C. Then, the membranes were exposed to secondary antibodies at RT for 1 h. The protein bands on the membranes were visualized using enhanced chemiluminescence (ECL) detection reagents (Santa Cruz Biotechnology, CA, USA).

Establishment of overexpression or knockdown cell lines

Control and STING-specific shRNA lentiviral particles were purchased from Gene Pharma (Shanghai, China). MC38 cells were transduced with four distinct lentiviral stocks using polybrene. Following transduction, stable cell lines expressing the shRNA constructs were selected with puromycin. For stable overexpression of PCSK9 and OVA, HEK293T cells were cotransfected with the following plasmids: 1.5 μg of pMD2. G, 3 μg of psPAX2 and 6 μg of the construct containing the specific gene of interest for overexpression. Lipofectamine 3000 was utilized as the transfection reagent. Viral particles were collected at both 24 h and 48 h posttransfection. To transduce the target cells, the harvested viral particles combined with polybrene were added. Stable clones were then selected using puromycin.

LDH release assay

LDH release was quantified using an LDH release assay kit (Promega) according to the manufacturer's instructions. Briefly, OVA-specific $CD8^+$ T cells were isolated from the spleens and lymph nodes of OT-I mice (the mice were kindly provided by Professor Wende Li from Guangdong Laboratory Animals Monitoring Institute). MC38-OVA cells (1×10^4) treated with or without 10 μM nilotinib for 48 h were seeded in 96-well plates, and then OT-I T cells were plated in 96-well plates at the effector/target ratios shown. After 12 h of incubation at 37 °C, 50 μL of supernatant from each well was incubated with the substrate for 30 min at room temperature. The release of LDH in the supernatant of each well was determined by measuring the absorbance at 490 nm with a 96-well plate reader (Thermo Fisher Scientific).

ELISA

ELISA kits were purchased from Multisciences (Hangzhou, Zhejiang, China). After 12 h of coculture, concentrations of IFNγ and TNFα in the supernatants were assessed using these kits following the manufacturer's guidelines.

Animal study

Male mice were obtained from GemPharmatech Co., Ltd. All animal experiments (IACUC-2020122502 and IACUC-2021110401) were conducted in accordance with the guidelines set by the Committee on the Ethics of Animal Experiments of the Sixth Affiliated Hospital, Sun Yat-sen University. This study employed two murine models, established as follows:

(1) CT-26 cells (1×10^5) were subcutaneously injected into BALB/c mice. Four days postinoculation, the mice were randomly assigned to four groups. For the method of drug administration, an anti-PDL1 antibody (BioXCell, Lebanon, NH, USA) was injected intraperitoneally (i.p.) at a dose of 5 mg/kg every 2 days. Nilotinib (Novartis, Basel, Basel-Stadt, Switzerland) was administered via oral gavage at 25 mg/kg daily.
(2) MC38 cells (2×10^5) were subcutaneously injected into C57BL/6 mice. Four days postinoculation, the mice were randomly assigned to four groups. For the method of drug administration, 1 mg/kg anti-PDL1 antibody was injected intraperitoneally (i.p.) every 2 days. Nilotinib was administered via oral gavage at 25 mg/kg daily. CD8a depletion antibody (BioXCell) was administered i.p. at 15 mg/kg every 3 days. Tumor dimensions were recorded every other day, and tumor volumes were calculated using the formula: $\text{Volume}=a^2\times b/2$, where a represents the smallest diameter and b is the diameter perpendicular to a. Finally, the mice were humanely euthanized. The excised tumors were weighed, photographed and retained for subsequent analyses.

RNA-seq analysis

Total RNA was extracted from both untreated HCT116 cells and HCT116 cells treated with 20 μM nilotinib for 24 h. RNA-seq analysis was conducted on the Illumina NovaSeq 6000 platform performed by NovelBio BioPharm Technology Co., Ltd. (Shanghai, China). Differentially expressed genes (DEGs) were defined with criteria of a fold change greater than or equal to ± 1 and a false discovery rate (FDR) < 0.01, calculated using RNA-seq by expectation–maximization and the Passion distribution methods. DEGs were subsequently subjected to KEGG pathway analysis for enrichment studies (http://www.genome.jp/kegg/pathway.html). Gene Set Enrichment Analysis (GSEA) was performed using the OECloud tools (https://cloud.oebiotech.com).

Detection of cytosolic DNA

HCT116 cells (1×10^7) were equally partitioned into two samples. For the first, cells were resuspended in 200 µL of 50 µM NaOH, boiled for 30 min, and then neutralized with 20 µL of 1 M Tris–HCl (pH 8), which served as a normalization control for total DNA. For the second, cells were resuspended in 200 µL of buffer (containing 150 mM NaCl, 50 mM HEPES and 25 µg/mL digitonin) and incubated for 10 min on ice to permeabilize the plasma membrane. Following this, centrifugation at 980 × g for 3 min was repeated three times to sediment intact cells. Subsequently, the cytosolic supernatants were centrifuged at 17,000 × g for 10 min to clear the cellular fragments. DNA from cytosolic and whole-cell DNA samples were purified using DNA Clean & Concentrator-5 (Zymo Research, Irvine, CA, USA). qRT–PCR was performed on both cytosolic samples using gDNA primers, with CT values from whole-cell extracts serving as a normalization for those from the cytosolic fractions.

Immunofluorescence assay

Cells were seeded on coverslips in 24-well plates. After nilotinib treatment, the cells were fixed with 4% paraformaldehyde for 20 min and blocked with 10% goat serum for 1 h. The cells were then probed with a primary anti-p-p65 antibody (1:100) overnight at 4 °C. This was followed by incubation with Alexa Fluor 488-conjugated secondary antibody (Thermo Fisher Scientific) for 1 h at room temperature. Nuclei were stained with Hoechst or DAPI for 10 min. Images were acquired using a Leica TCS-SP8 laser confocal microscope (Leica, Mannheim, Baden-Wuerttemberg, Germany).

Tissue chip microarray

A tissue microarray chip (HColA180Su12) comprising 93 human colon cancer tissues and 87 adjacent normal tissues was purchased from Shanghai Outdo Biotech. 2 colon cancer tissues and 11 adjacent normal tissues were unable to evaluate due to destroyed or incomplete tissues. PCSK9 expression was assessed using an anti-PCSK9 antibody at a dilution of 1:1000 through immunohistochemical analysis. The microarray was scanned using a Leica SCN400 slide scanner (Leica). Scoring of PCSK9 expression was performed by clinical pathologists.

Statistical analysis

The data are presented as the mean ± SD, and were derived from a minimum of three independent experiments. Analysis was conducted using GraphPad Prism 8.0 software (San Diego, CA, USA). Significance was determined using Student's *t* test between two groups or one-way analysis of variance (ANOVA) with Tukey's multiple comparison test for multiple group comparisons. Kaplan–Meier analysis and log-rank tests were used for survival analysis. The chi-square test was used to analyze the correlation between the PCSK9 expression level and clinical pathological characteristics in Table 1. A P value < 0.05 was considered to indicate statistical significance.

Table 1 The correlation between the PCSK9 expression level and clinical pathological characteristics

Factors	Number of cases (n)	PCSK9		*p*
		Low	High	
Number	91	51	40	
Age (years)				0.428
< 60	29	18	11	
≥ 60	62	33	29	
Gender				0.206
Female	50	31	19	
Male	41	20	21	
T classification				0.133
T1 + T2	5	5	0	
T3 + T4	78	43	35	
Unknown	8	3	5	
N classification				0.040
N0	50	32	18	
N1 + N2	36	15	21	
Unknown	5	4	1	
Metastasis				0.790
No	87	48	39	
Yes	4	3	1	
Tumor stage				0.018
I + II	44	30	14	
III + IV	38	16	22	
Unknown	9	5	4	

p values derived from the Chi-square test

Results

Nilotinib induces MHC-I expression in CRC cells

To identify promising drug candidates that can increase MHC-I expression in CRC cells, we screened a library of 238 FDA-approved drugs using the HLA-A2 luciferase screening system. We found that 9 drugs exhibited a fold change in luciferase activity greater than 2 (Fig. 1A). Then, the effects of these 9 drugs on MHC-I mRNA levels were confirmed by using RT-qPCR, and our results showed that nilotinib achieved the greatest upregulation of MHC-I mRNA levels (Fig. 1B). To verify the effects of nilotinib on the upregulation of MHC-I in CRC, we first measured MHC-I luciferase activity at various doses of nilotinib in multiple human CRC cell lines. As shown in

Fig. 1C, nilotinib significantly enhanced MHC-I luciferase activity in CRC cells. RT-qPCR analysis revealed that HLA-A and β2M mRNA levels increased in HCT116 and SW480 cells with nilotinib treatment (Fig. 1D). Furthermore, Nilotinib increased the protein expression of HLA-A and β2M in HCT116 and SW480 cells detected by both flow cytometry and western blot analysis (Fig. 1E and F). Taken together, these data indicate that nilotinib increases MHC-I expression in CRC cells at both the mRNA and protein levels.

Nilotinib enhances the antitumor effects of anti-PDL1 by increasing MHC-I expression in CRC cells and enhancing $CD8^+$ T-cell cytotoxicity

To explore whether nilotinib-induced MHC-I upregulation in CRC cells directly affects the cytotoxicity of $CD8^+$ T cells, we generated MC38 cell lines stably expressing ovalbumin (OVA) peptide (SIINFEKL) (MC38-OVA). These cell lines are recognized by $CD8^+$ T cells from OT-I mice owing to their OVA antigen specificity [25]. IFNγ has been reported to increase the expression of SIINFEKL-H-2 Kb [14]. Intriguingly, we found that the expression level of SIINFEKL-H-2 Kb was higher after nilotinib treatment than after IFNγ treatment (Fig. 2A). We then performed a lactate dehydrogenase (LDH) assay to determine T-cell cytotoxicity and used ELISA to measure IFNγ and TNFα levels by coculturing MC38-OVA cells with $CD8^+$ T cells from OT-I mice. Compared with control, OT-I T cells cocultured with nilotinib-treated MC38-OVA cells exhibited greater cytotoxicity and secreted much higher levels of IFNγ and TNFα (Fig. 2B and C). These results suggest that nilotinib strongly induces the presentation of the MHC-I peptide antigen, thereby enhancing $CD8^+$ T-cell-mediated cytotoxicity in vitro.

Enhancing MHC-I expression in cancer cells is a promising strategy to improve ICI efficacy [12]. As nilotinib increases MHC-I levels and directly enhances $CD8^+$ T-cell-mediated cytotoxicity in vitro, we hypothesized that nilotinib could increase the efficacy of anti-PDL1 therapy in vivo. To test this hypothesis, we utilized subcutaneous MC38 and CT26 tumor models, which have been validated as microsatellite instability (MSI) and microsatellite stability (MSS) models of CRC, respectively [26]. C57BL/6 mice were inoculated with MC38 cells and then injected with vehicle, a low dose of nilotinib, a low dose of anti-PDL1 antibody, or a combination of both nilotinib and anti-PDL1 antibody. As shown in Fig. 2D–F, although neither low-dose nilotinib nor the anti-PDL1 antibody significantly inhibited tumor growth, the combination of nilotinib and the anti-PDL1 antibody dramatically suppressed tumor volume and tumor weight. Moreover, the expression of H-2 kb was markedly increased in both the nilotinib alone group and the combined drug treatment group. (Fig. 2G). In addition, although the percentage of total $CD8^+$ T cells increased in both the PDL1 antibody alone group and the combined drug treatment group, the percentage of $IFN\gamma^+$ $CD8^+$ T cells was significantly higher only in the combined drug treatment group (Fig. 2H and I). Similarly, nilotinib also increased $H\text{-}2k^d$ expression and enhanced anti-PDL1 efficacy in the CT26 tumor model (Additional file 1: Fig. S1). These results demonstrate a synergistic effect between nilotinib and ICIs in both MSI-high and MSS CRC models.

To further determine the role of effector T cells in the antitumor effects of combined drug treatment, we used anti-CD8 antibody to deplete $CD8^+$ T cells in C57BL/6 mice, and $CD8^+$ T-cell depletion abrogated the efficacy of combined drug treatment (Fig. 2J–L). All of these results suggest that nilotinib boosts the efficacy of anti-PDL1 therapy by upregulating MHC-I expression in CRC cells and increasing $CD8^+$ T-cell cytotoxicity.

Nilotinib increases MHC-I expression by activating the NF-kB pathway

We then investigated the molecular mechanisms of nilotinib-induced MHC-I expression in CRC cells. As nilotinib is a small molecule that selectively inhibits the tyrosine kinase activity of the oncogene ABL, we wondered whether nilotinib increases MHC-I expression by regulating the tyrosine kinase activity of ABL. However, we found that MHC-I expression in CRC cells remained unaffected when we used other ABL inhibitors, including bosutinib and ponatinib, to treat CRC cells (Additional file 1: Fig. S2), indicating the existence of other molecular mechanisms. Given that nilotinib affects MHC-I expression at the RNA level, RNA-seq analysis was performed to investigate the possible signaling pathways that

(See figure on next page.)

Fig. 1 Nilotinib upregulates MHC-I expression in CRC cells. **A** Luciferase activity of HLA-A2 in HCT116 cells treated with 238 FDA approved drugs at the concentration of 10 μM for 24 h. **B** The MHC-I mRNA levels in HCT116 cells treated with 9 candidate drugs at the concentration of 10 μM for 24 h. **C** Luciferase activity of HLA-A2 and β2M in HCT116 and SW480 cells after 24 h and 48 h of nilotinib treatment, respectively. **D** The mRNA expression of HLA-A and β2M in HCT116 and SW480 cells after 24 h and 48 h of nilotinib treatment, respectively. **E** and **F** The protein expression of HLA-A and β2M in HCT116 and SW480 cells after 24 h and 48 h of nilotinib treatment, respectively. The results are shown as the mean ± SD. ns. $P > 0.05$, *$P < 0.05$, **$P < 0.01$, ***$P < 0.001$, ****$P < 0.0001$, versus the control group

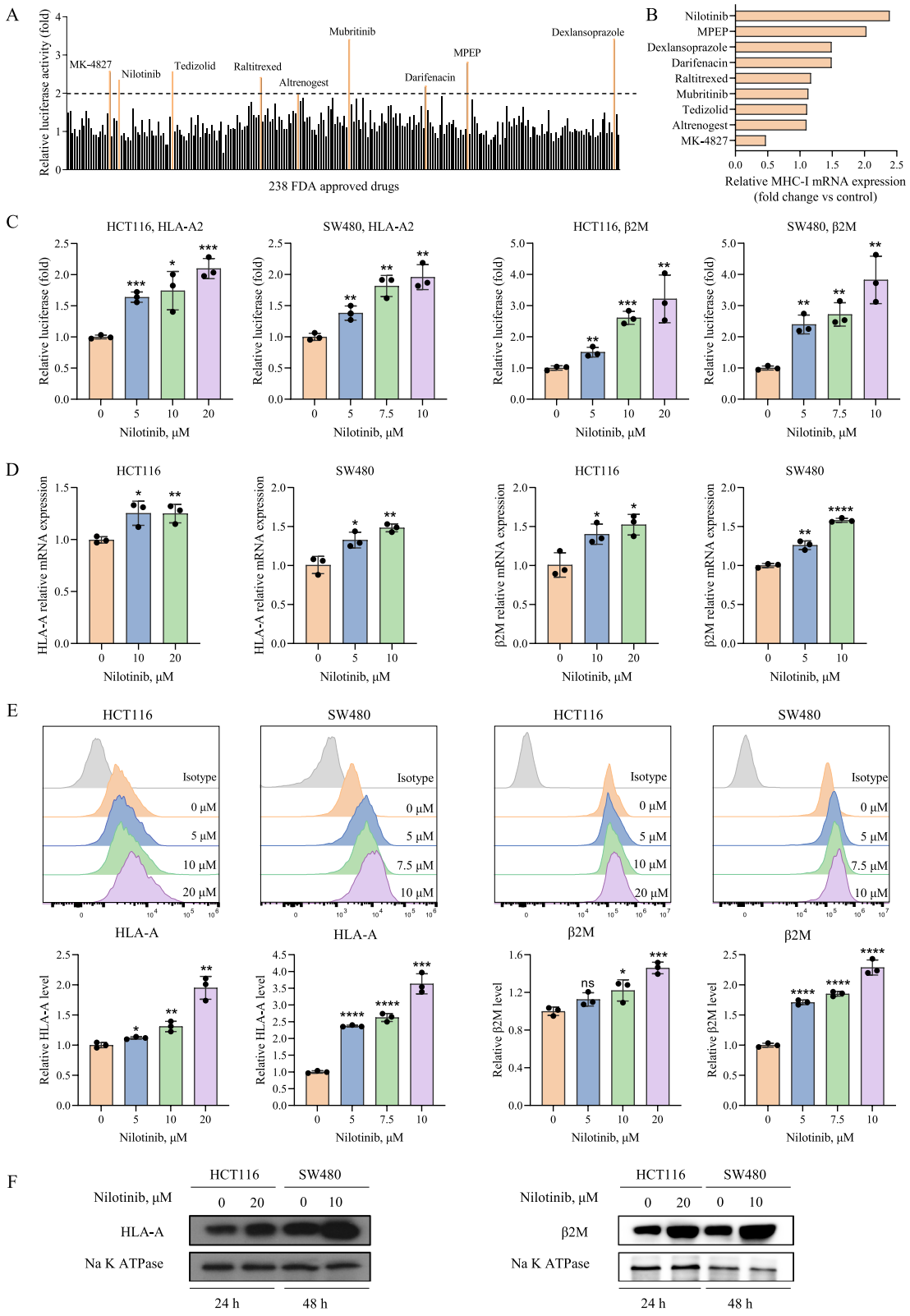

Fig. 1 (See legend on previous page.)

regulate the expression of MHC-I in CRC. Several pathways were changed after nilotinib treatment, and one of the most enriched pathways was the NF-κB signaling pathway (Fig. 3A). Gene set enrichment analysis (GSEA) confirmed that nilotinib significantly activated the NF-κB signaling pathway (Fig. 3B). Previous reports have indicated that activation of the NF-κB signaling pathway participates in the induction of MHC-I antigen presentation in prostate cancer cells [27]. The NF-κB signaling pathway was selected for further study. In line with the RNA-seq results, we verified that nilotinib indeed enhanced the transcriptional activity of NF-κB and significantly increased the protein levels of p65 and p-p65 (Fig. 3C–E). Moreover, nilotinib promoted p-p65 translocation from the cytoplasm to the nucleus (Fig. 3F). Interestingly, when NF-κB activation was blocked by the NF-κB inhibitor JSH-23, the nilotinib-induced upregulation of MHC-I was partly abrogated in CRC cells (Fig. 3G). Together, these results indicate that the NF-κB signaling pathway is involved in the upregulation of nilotinib-induced MHC I expression in CRC cells.

Nilotinib-induced MHC-I upregulation is mediated by the cGAS-STING-NF-κB *axis*

We further investigated the mechanisms by which nilotinib activates the NF-κB pathway. The RNA-seq results revealed that the cytosolic DNA sensing pathway was enriched in CRC cells treated with nilotinib (Fig. 4A). Moreover, nilotinib treatment led to micronuclei formation and increased the amount of cytosolic genomic DNA (gDNA) (Fig. 4B and C). The cGAS-STING pathway can be activated by the sensing of cytosolic DNA, and the activated STING pathway subsequently activates NF-kB, which has been reported to be critical for MHC-I expression [28–31]. Therefore, we wondered whether the STING pathway initiates NF-κB activation followed by MHC-I upregulation. As shown in Fig. 4D, nilotinib markedly increased the level of STING phosphorylation, indicating that the STING pathway was activated by nilotinib. When STING activation was blocked by the STING inhibitor H151, the nilotinib-induced activation of NF-κB was abrogated in CRC cells (Fig. 4E). These findings illustrate that nilotinib activates NF-κB through the cGAS-STING pathway. We next explored whether STING is required for nilotinib-induced MHC I upregulation by flow cytometry. The results demonstrated that the nilotinib-induced increase in MHC-I expression was partly reversed by cotreatment with the STING inhibitor H151 (Fig. 4F).

As STING signaling is involved in the nilotinib-induced activation of NF-kB and subsequent upregulation of MHC-I expression in CRC cells, we then tested whether STING signaling is required for the tumor inhibition induced by the combination of nilotinib and anti-PDL1 antibody. We first generated stable STING-knockdown MC38 cells (MC38-shSTING) (Fig. 4G). MC38-shSTING-1 cells, which exhibited low STING expression, were used for in vivo investigations. MC38-shVC (vehicle control) and MC38-shSTING-1 cells were injected subcutaneously into C57BL/6 mice, which were treated with or without the combination of nilotinib and ani-PDL1 antibody. Combined drug treatment significantly inhibited tumor growth in the shVC group, while inhibitory effects were undetectable in the shSTING-1 group (Fig. 4H–J). In addition, STING knockdown inhibited the upregulation of H-2 kb expression induced by combination therapy (Fig. 4K). Together, these results indicate that nilotinib enhances MHC-I expression by activating the cGAS-STING-NF-κB axis.

Nilotinib attenuates MHC-I degradation by decreasing PCSK9 expression

Functional loss at various stages of MHC-I antigen presentation has been implicated as an important immune evasion strategy, leading to resistance to ICIs [32, 33]. Our RT-qPCR results revealed a slight increase in the MHC-I transcript level after nilotinib treatment, while flow cytometry revealed significant upregulation of the MHC-I protein. Therefore, we wondered whether nilotinib regulates MHC-I expression through protein translation or degradation. Previous research has shown that PCSK9, a key protein in the regulation of cholesterol

(See figure on next page.)

Fig. 2 Nilotinib augments anti-PDL1 efficacy by enhancing MHC-I expression and amplifying $CD8^+$ T-cell-mediated cytotoxicity. **A** Expression of SIINFEKL-H-2 Kb in MC38-OVA cells following treatment with either 10 μM nilotinib for 48 h or 5 ng/mL IFNγ for 24 h. Subsequently, the MC38-OVA cells treated with 10 μM nilotinib for 48 h were cocultured with OT-I T cells for 12 h, after which the supernatant was collected. **B** T-cell cytotoxicity was determined by LDH release assay. **C** IFNγ and TNFα levels were determined by ELISA. **D** In C57BL/6 mice bearing MC38 xenografts and treated with anti-PDL1 antibody (i.p., 1 mg/kg, every 2 days), nilotinib (orally, 25 mg/kg, daily) or both (N + P), tumor volumes were monitored every other day. **E** and **F** After sacrifice, the tumors were weighed and imaged. **G** H-2 Kb expression levels in tumor samples. **H** Percentage of $CD8^+$ T cells among tumor-infiltrating lymphocytes. **I** Proportion of $IFN\gamma^+$ cells within the $CD8^+$ T-cell population. **J** In another cohort of C57BL/6 mice bearing MC38 xenografts and treated with the anti-PDL1 antibody, nilotinib, and with or without the CD8a antibody (i.p., 15 mg/kg, every 3 days), tumor volumes were monitored every other day. **K** and **L** Following sacrifice, the tumors were weighed and imaged. The results are shown as the mean ± SD. ns. $P > 0.05$, $^*P < 0.05$, $^{**}P < 0.01$, $^{***}P < 0.001$, $^{****}P < 0.0001$

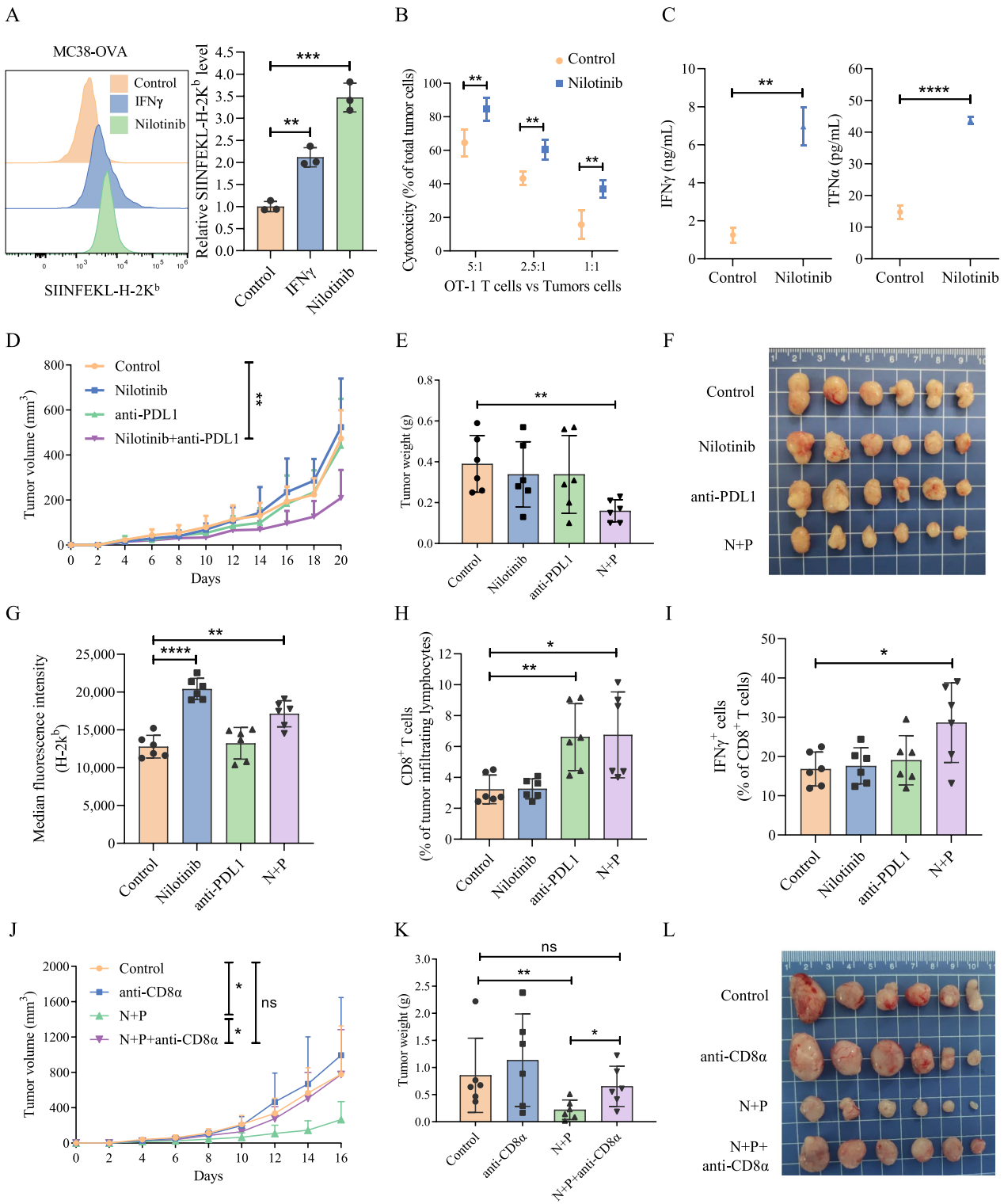

Fig. 2 (See legend on previous page.)

metabolism, can promote lysosomal MHC I degradation and influence the tumor immune response [34, 35]. Therefore, we examined whether nilotinib-induced cell-surface MHC-I upregulation is associated with PCSK9 expression. HCT116 and SW480 cells were exposed to nilotinib, and the effects of nilotinib on

PCSK9 protein levels were assessed by western blotting. Our results showed that PCSK9 protein expression was inhibited in the presence of nilotinib (Fig. 5A). Moreover, overexpression of PCSK9 in CRC cells reversed nilotinib-induced MHC I upregulation (Fig. 5B and C).

Considering our in vitro findings, we further explored the role of PCSK9 in combination therapy-mediated inhibition of tumor growth. MC38 cells stably overexpressing PCSK9 or vector (Fig. 5D) were inoculated into the flanks of C57BL/6 mice. Indeed, the overexpression of PCSK9 reversed the inhibitory effect on the tumor volume and weight caused by combination treatment with nilotinib and the anti-PDL1 antibody (Fig. 5E–G). Consistent with the in vitro results, H-2 kb upregulation in subcutaneously transplanted tumors induced by combination therapy was impaired after overexpressing PCSK9 (Fig. 5H). These data suggest that in addition to upregulating MHC I expression at the transcriptional level, nilotinib regulates MHC-I internalization and degradation via PCSK9.

PCSK9 expression levels in CRC specimens and prognostic value

PCSK9 has been reported as a therapeutic target for atherosclerotic cardiovascular diseases [36]. Recently, increasing evidence has shown that PCSK9 plays an important role in tumor development and may be a potential therapeutic target for tumor therapy [37–39]. Therefore, we evaluated the clinical relevance of PCSK9 in CRC and explored the potential of PCSK9 as a treatment target in CRC. We first assessed PCSK9 transcript expression in a TCGA pancancer dataset obtained from the Gene Expression Profiling Interactive Analysis (GEPIA) online database, and the data revealed that PCSK9 was abnormally expressed in different cancers (Fig. 6A). In colon adenocarcinoma (COAD) tissue, the expression of PCSK9 was strikingly greater than that in healthy tissue (Fig. 6B). To further confirm PCSK9 expression in CRC specimens, IHC staining was performed on a clinical tissue microarray chip that included tumor tissues and normal tissues. As shown in Fig. 6D and E, COAD tissues presented higher PCSK9 expression than normal tissues. Then we analyzed the correlation of PCSK9 expression with clinical pathological parameters. Although, expression of PCSK9 was not associated with age, gender, T classification and metastasis of CRC patients, high PCSK9 expression was significantly associated with advanced N classification and tumor stage (Table 1). We further evaluated the prognostic value of PCSK9 using clinical survival data from GSE17538 dataset and tissue microarrays. The results showed that patients with lower PCSK9 expression had a better prognosis in the COAD cohorts (Fig. 6C and F). These results demonstrate that PCSK9 may serve as a potential therapeutic target for CRC patients, and further suggest that nilotinib, which inhibits PCSK9 expression in CRC cells, is a potential candidate for CRC treatment.

Discussion

ICIs have shown promising clinical benefits in CRC patients with dMMR/MSI-H [4]. However, only 15% of CRC patients are dMMR/MSI-H and not all these patients respond to ICIs [5, 6]. It has been reported that pembrolizumab, a PD-1 inhibitor, resulted in an objective response rate of only 52% in patients with MSI-H/dMMR CRC [40]. Thus, strategies to enhance the efficacy of ICIs for CRC treatment are urgently needed. Insufficient antigen presentation to activate $CD8^+$ T cells represents one of the major reasons why ICIs are ineffective [41]. Enhancing MHC-I expression in tumor cells helps to improve antigen presentation and is an efficient strategy for facilitating ICIs [8, 42]. Given the substantial safety and efficacy of FDA-approved medications, we screened an FDA-approved drug library to identify compounds that enhance MHC-I expression. In the present study, our results showed that nilotinib induces the expression of MHC-I, promotes $CD8^+$ T-cell activation and potentiates anti-PDL1 efficacy.

Nilotinib, which is used to treat chronic myelogenous leukemia, has been found to exert antitumor effects on solid tumors [20–24]. Clinical studies have also shown the significant efficacy of nilotinib in patients with metastatic malignant melanoma harboring kit gene aberrations and

(See figure on next page.)

Fig. 3 The NF-κB signaling pathway is involved in nilotinib-induced MHC I upregulation in CRC cells. RNA-seq analysis was conducted on HCT116 cells, both untreated and treated with 20 μM nilotinib for 24 h. **A** KEGG pathway enrichment analysis based on the differentially expressed genes. **B** GSEA plots showing enrichment of the NF-κB signaling pathway in nilotinib-treated HCT116 cells versus controls. **C** Luciferase activity indicating NF-κB activation in HCT116 and SW480 cells after nilotinib treatment for 24 h and 48 h, respectively. **D** Expression profiles of total p65 and its phosphorylated form (p-p65) in HCT116 and SW480 cells after nilotinib treatment at various concentrations. **E** Nuclear p65 expression in HCT116 and SW480 cells with or without nilotinib treatment. **F** Cellular distribution of p-p65 in HCT116 and SW480 cells treated with nilotinib for 24 h and 48 h, respectively; the scale bar represents 25 μm. **G** HCT116 cells were pretreated with 20 μM JSH-23 for 2 h, followed by cotreatment with 20 μM nilotinib for an additional 24 h. Similarly, SW480 cells were pretreated with 10 μM JSH-23 for 2 h and cotreated with 10 μM nilotinib for 48 h. Subsequent HLA-A expression was analyzed using flow cytometry. The results are shown as the mean ± SD. $^*P < 0.05$, $^{***}P < 0.001$, $^{****}P < 0.0001$

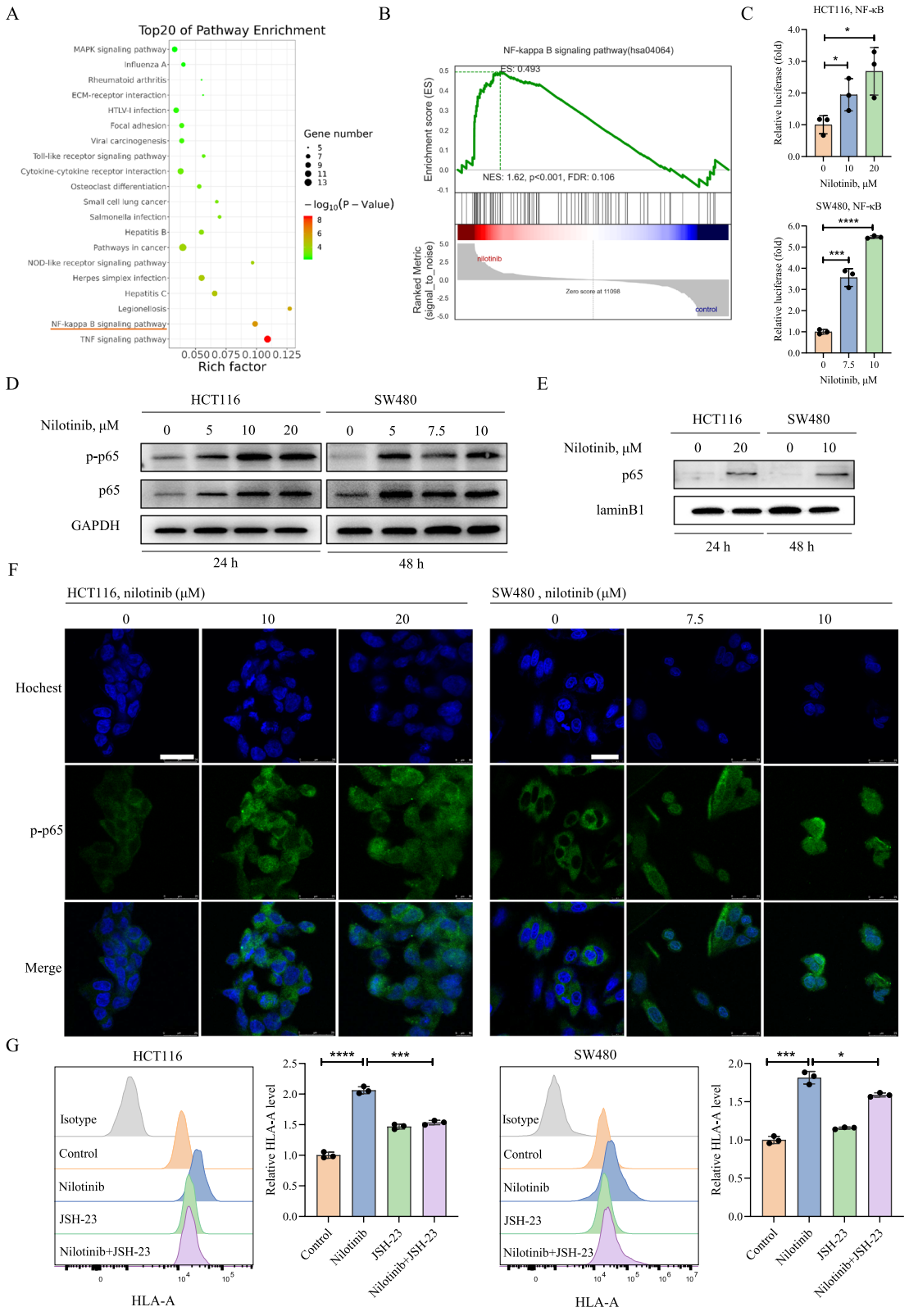

Fig. 3 (See legend on previous page.)

patients with gastrointestinal stromal tumors resistant or intolerant to imatinib and sunitinib [43, 44]. Moreover, it has been reported that nilotinib inhibits CRC metastasis by targeting DDR1-BCR signaling, suggesting the potential of nilotinib as a therapeutic drug for CRC patients [45]. However, whether nilotinib affects antitumor immunity in CRC remains uncertain. In this study, the results showed that nilotinib induces MHC-I surface expression in CRC cells and thus promotes $CD8^+$ T-cell activation. $CD8^+$ T cells are crucial in anti-tumor immunity, and the secretion of TNFα and IFNγ is the important indicator of $CD8^+$ T cell activation [46]. Here, we found nilotinib treatment markedly increased the release of cytotoxic cytokine IFNγ from $CD8^+$ T cells in vitro and in vivo. IFNγ signaling could directly affect tumor cell viability and enhance tumor antigen presentation followed by boosting T cell-mediated killing of tumor cells [47]. The essential role of IFNγ signaling pathway in immunotherapy has been experimentally proven. Ayers et al. showed active IFNγ signaling is a common feature of tumors that respond to ICIs [48]. Conversely, defects in IFNγ signaling are related to immunotherapy resistance [49]. Results from this study and previously reported findings suggest that nilotinib-induced IFNγ secretion plays an important role in enhancing anti-PDL1 efficacy.

We next investigated how nilotinib affects the expression of MHC-I. While nilotinib has been reported to be an ABL inhibitor, it is important to note that other ABL inhibitors, such as bosutinib and ponatinib, did not increase MHC-I expression, indicating that ABL signaling might not be involved in this process. To understand the molecular mechanisms underlying the nilotinib-mediated regulation of MHC-I expression, RNA-seq was performed. Here, for the first time, we report that nilotinib activates the NF-κB signaling pathway in CRC cells. Importantly, the NF-κB pathway has previously been confirmed to be involved in the regulation of MHC-I gene expression [50, 51]. Zhou et al. demonstrated that activation of NF-κB can potentiate cancer chemoimmunotherapy via induction of MHC-I antigen presentation [27]. Consistently, we found that nilotinib upregulates the expression of MHC-I by activating the NF-κB signaling pathway.

After identifying the role of NF-κB in nilotinib-mediated MHC-I upregulation, we wanted to explore the upstream signaling pathways that activate NF-κB. The abundance of micronuclei and gDNA in the cytoplasm significantly increased after nilotinib treatment. Considering that the cGAS/STING pathway is known as a cytoplasmic DNA sensor, we hypothesized that the accumulation of cytosolic DNA induced by nilotinib activates the cGAS-STING pathway. Some recent studies have demonstrated the role of the cGAS-STING pathway in regulating the expression level of MHC-I [29, 31]. In addition, Caiazza et al. showed that the absence of STING impairs MHC-I-dependent antigen presentation [52]. Given that NF-κB is one of the most important downstream pathways of the cGAS/STING pathway [30], our results show that nilotinib promotes MHC-I expression by activating the cGAS-STING-NF-κB axis. Moreover, the cGAS/STING pathway can also promote type I interferon (IFN) production via IRF3 activation. Type I IFN is known to promote the activation and maturation of dendritic cells followed by facilitating $CD8^+$ T-cell cross-priming [53, 54]. Similarly, we also observed the activation of $CD8^+$ T cells after nilotinib treatment. Therefore, we speculate that type I IFN-mediated dendritic cell maturation may be involved in nilotinib-induced $CD8^+$ T-cell activation. Further experiments are required to confirm this hypothesis in the future.

Given that nilotinib slightly elevates MHC-I expression at the transcriptional level, we further explored the effects of nilotinib on MHC-I internalization and degradation. The lysosomal degradation of MHC-I molecules leads to decreased cell membrane abundance and consequent inhibition of $CD8^+$ T-cell antitumor activity [55–57]. Our results showed that PCSK9 expression was reduced after nilotinib treatment. PCSK9 is known to promote the degradation of low-density lipoprotein receptors, which are essential for lowering cholesterol levels [58]. PCSK9 inhibitors have been used to treat hypercholesterolemia and related cardiovascular diseases

(See figure on next page.)

Fig. 4 Nilotinib elevates MHC-I expression via the cGAS-STING-NF-κB signaling pathway. **A** GSEA enrichment plots of the cytosolic DNA sensing pathway in nilotinib-treated HCT116 cells relative to controls. **B** Representative confocal images of DAPI-stained HCT116 cells treated with or without 20 μM nilotinib for 24 h; the scale bar represents 10 μm. **C**. Analysis of cytosolic gDNA content in HCT116 cells treated with or without 20 μM nilotinib for 24 h. **D** The expression of STING and p-STING in HCT116 and SW480 cells following nilotinib treatment at the indicated concentrations. Subsequently, HCT116 cells were pretreated with 1 μM H151 for 2 h and then cotreated with 15 μM nilotinib for another 24 h. SW480 cells were pretreated with 1 μM H151 for 2 h followed by cotreatment with 10 μM nilotinib for 48 h. **E** Analysis of p-p65 expression using western blotting. **F** HLA-A expression assessment using flow cytometry. **G** Verification of STING knockdown in MC38 cells at both the mRNA and protein levels. **H** Regular monitoring of tumor volume every other day. **I** and **J** Tumors harvested from euthanized mice were weighed and photographed. **K** Expression levels of H-2 Kb in tumor samples. The results are shown as the mean ± SD. $^*P < 0.05$, $^{**}P < 0.01$, $^{***}P < 0.001$, $^{****}P < 0.0001$ versus control

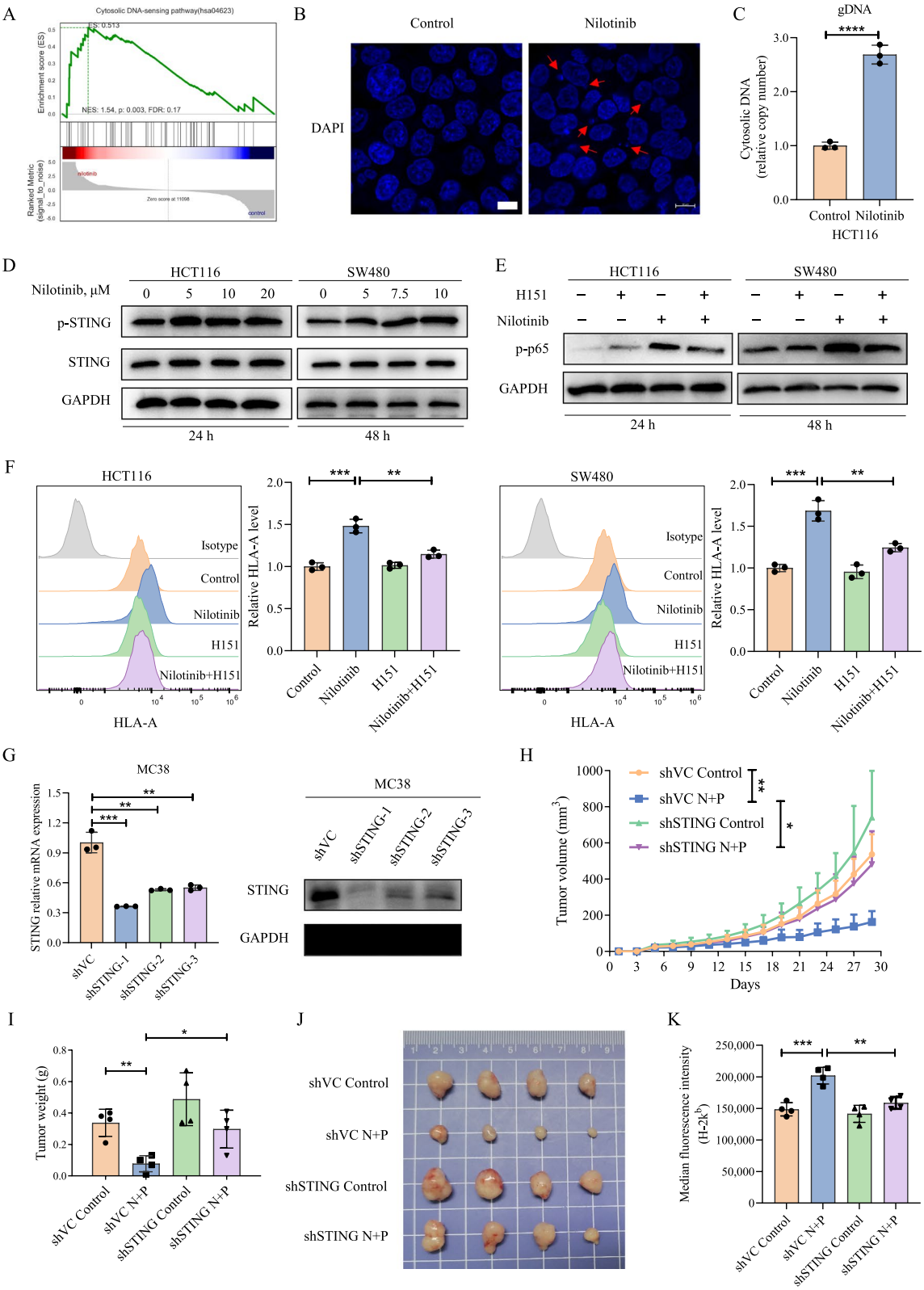

Fig. 4 (See legend on previous page.)

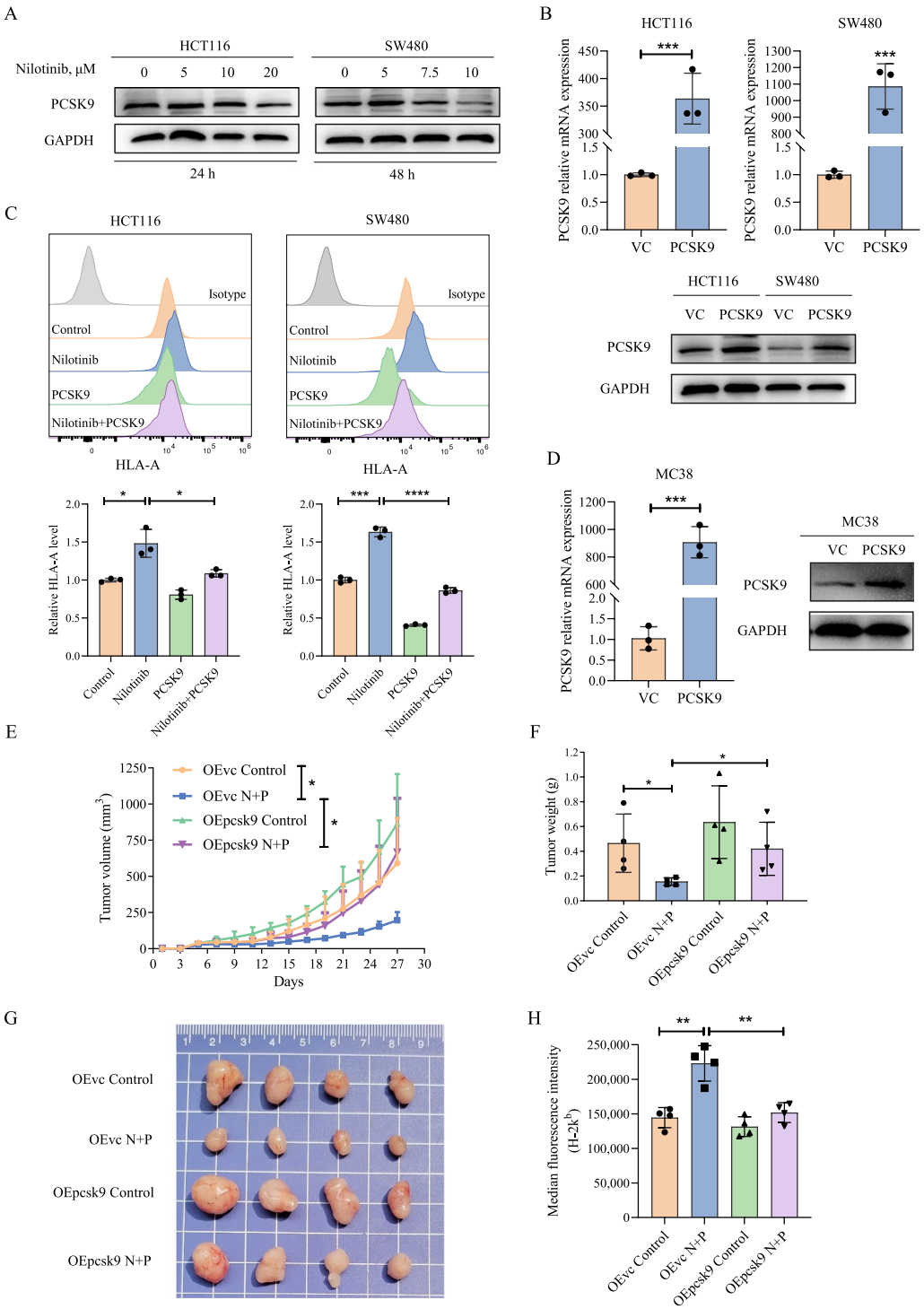

Fig. 5 Nilotinib attenuates MHC-I degradation by inhibiting PCSK9 expression. **A**. PCSK9 expression in HCT116 and SW480 cells treated with various concentrations of nilotinib. **B**. Verification of PCSK9 overexpression in HCT116 and SW480 cells at both the mRNA and protein levels. **C**. HCT116 cells overexpressing PCSK9 (or control vector) were treated with 15 μM nilotinib for 24 h, while SW480 cells overexpressing PCSK9 (or vector control) were treated with 7.5 μM nilotinib for 48 h. HLA-A expression was assessed using flow cytometry. **D**. PCSK9 overexpression in MC38 cells was validated at the mRNA and protein levels. E. Tumor sizes were monitored every other day. **F** and **G**. At the time of sacrifice, the tumors were weighed and photographed. **H**. Expression levels of H-2 Kb in tumor samples. The results are shown as the mean ± SD. *$P < 0.05$, **$P < 0.01$, ***$P < 0.001$, ****$P < 0.0001$

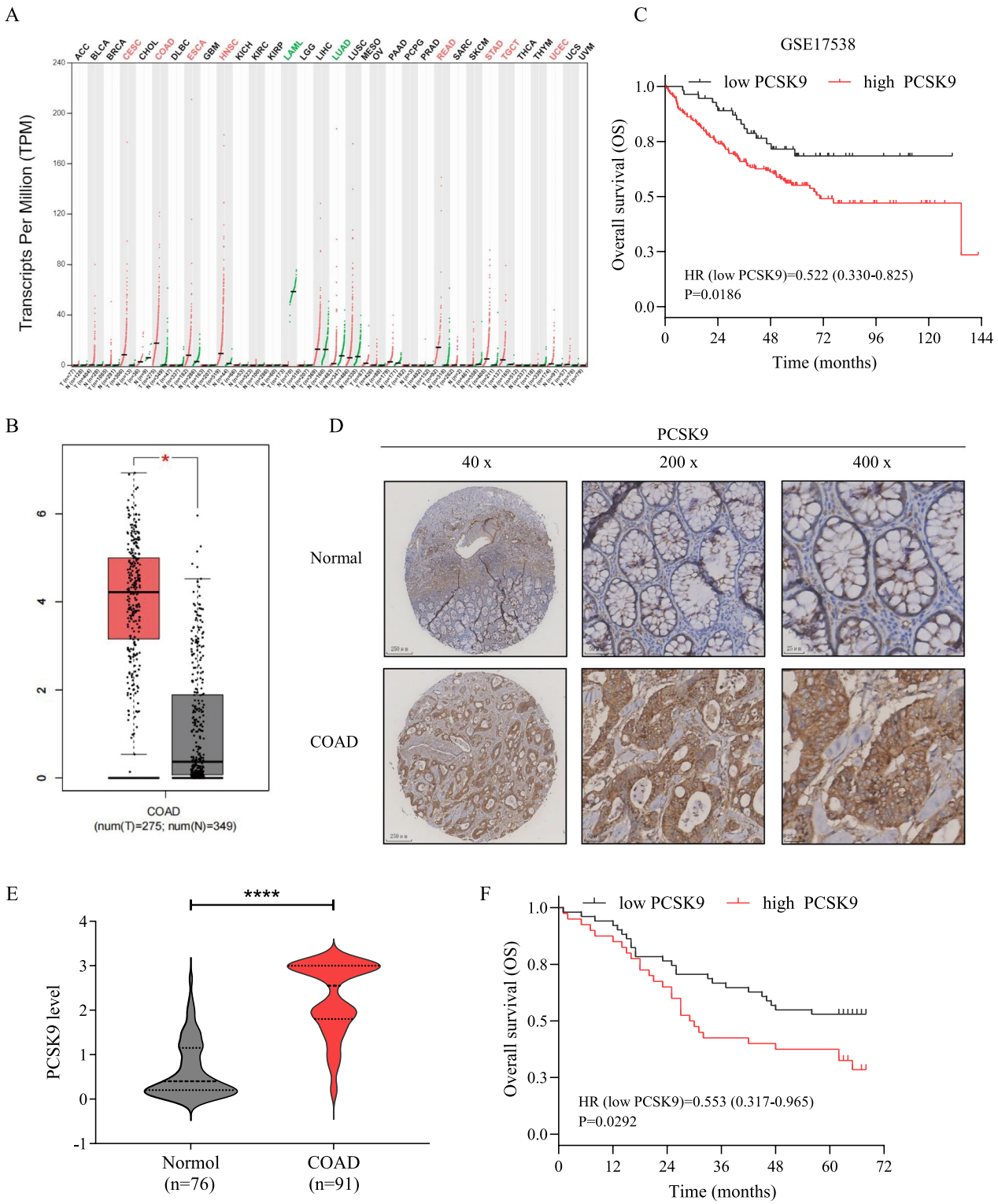

Fig. 6 PCSK9 expression and its prognostic value in CRC specimens. **A** Analysis of PCSK9 expression across various cancers using the GEPIA online database. **B** PCSK9 expression in COAD tissues, as determined by the GEPIA online database. **C** Kaplan–Meier survival analysis of 232 colon cancer patients stratified by PCSK9 expression according to clinical survival data from GSE17538 dataset. **D**.Comparison of PCSK9 expression in COAD and adjacent normal tissues. **E** Quantification of PCSK9 expression in the COAD tissue microarray. **F** Kaplan–Meier survival analysis of 91 COAD patients stratified by PCSK9 expression according to the tissue microarrays. The results are shown as the mean ± SD. *$P < 0.05$, ****$P < 0.0001$

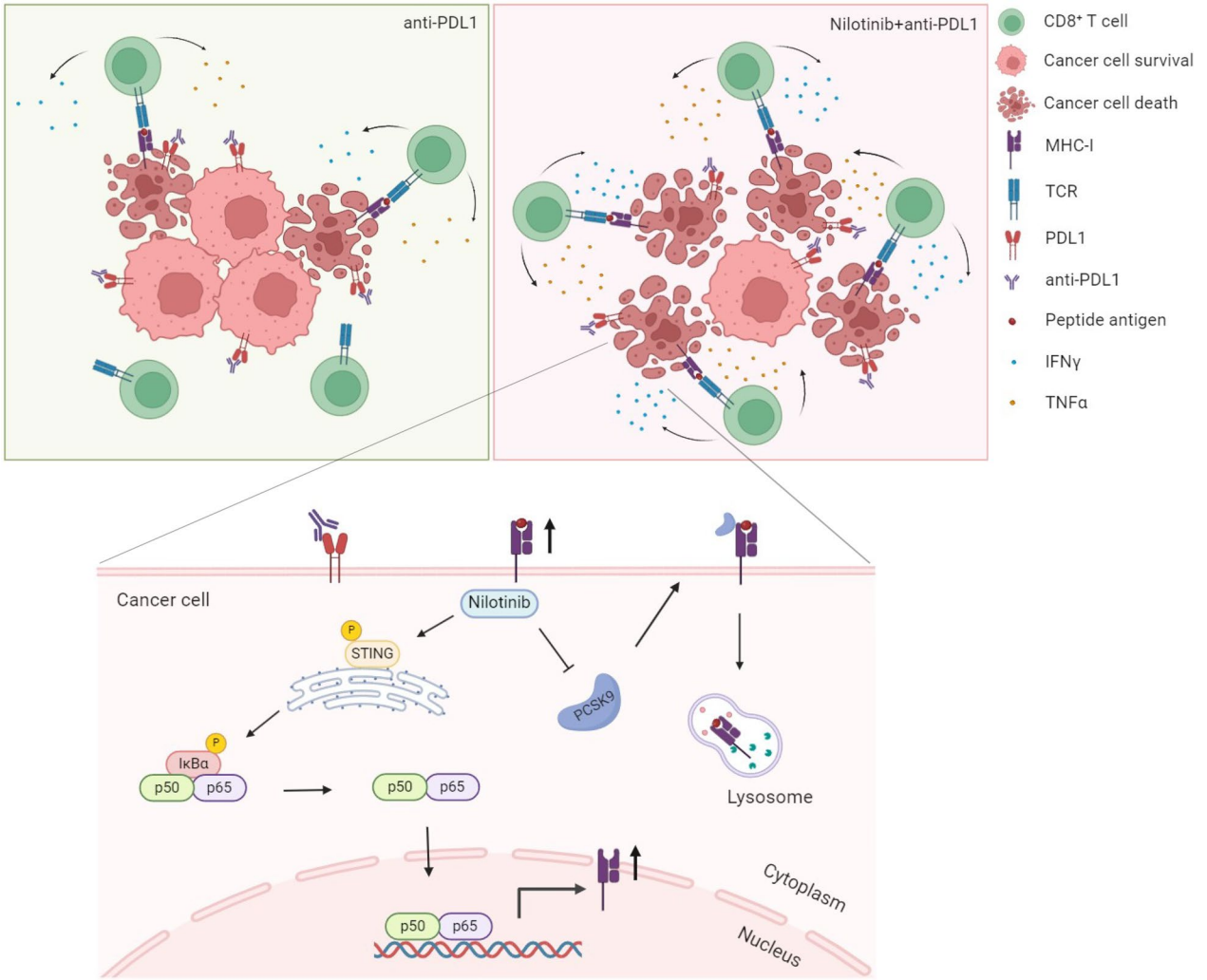

Fig. 7 Schematic diagram of the anti-CRC effects of nilotinib on CRC cells. (Drawing by BioRender (https://app.biorender.com/)). Nilotinib upregulates MHC-I expression via cGAS-STING-NF-κB activation and PCSK9 suppression, promotes the activation of $CD8^+$ T cells, and thus boosts the efficacy of anti-PDL1 therapy

[36]. Recently, targeting PCSK9 has been found to exert antitumor effects in several cancer types [37–39]. Importantly, Liu et al. demonstrated that the inhibition of PCSK9 leads to diminished MHC-I degradation in lysosomes and enhances tumor antigen presentation [34]. In this study, we observed that inhibiting PCSK9 with nilotinib increases the expression of MHC-I on the CRC cell surface. Previous studies have shown that dengue virus infection induces the expression of PCSK9, which results in STING inactivation [59]. Our results demonstrated that nilotinib upregulates MHC-I expression by activating the cGAS-STING-NF-κB axis. Therefore, in addition to inhibiting MHC-I degradation, the suppression of PCSK9 expression by nilotinib may also lead to the upregulation of MHC-I expression through STING activation. A recent study indicated that the expression of PCSK9 correlates with the survival of APC/KRAS-mutant CRC patients [60]. Our results also showed that the expression of PCSK9 is significantly greater in CRC tissues than in normal tissues and that CRC patients with lower PCSK9 expression have a better prognosis. Furthermore, nilotinib-induced PCSK9 inhibition enhances $CD8^+$ T-cell activation and the efficacy of anti-PDL1 therapy by increasing MHC-I surface expression in CRC. Therefore, PCSK9 may serve as a potential therapeutic target for CRC, and nilotinib targets PCSK9 to exert anti-CRC effects.

Despite these encouraging results, our study still has some limitations that require further research. First, more evidence is needed to demonstrate that nilotinib

enhances NF-κB activity and subsequently upregulates MHC-I expression in CRC cells. Second, the NF-κB pathway is a powerful cell survival factor in cancer cells [61]. Future studies should clarify the role of nilotinib-induced NF-κB activation in CRC progression. Third, the results shown in this study are preliminary, and further preclinical and clinical experiments are needed to validate the anti-CRC effects of nilotinib.

Conclusions

In summary, this study suggests that nilotinib could activate $CD8^+$ T cells, and thus boost the efficacy of anti-PDL1 therapy. These effects are probably mediated by cGAS-STING-NF-κB activation and PCSK9 suppression to upregulate MHC-I surface expression in CRC cells (Fig. 7). Therefore, combining nilotinib with anti-PDL1 therapy may represent a potential strategy for the treatment of CRC.

Abbreviations

ICIs	Immune checkpoint inhibitors
CRC	Colorectal cancer
MHC-I	Major histocompatibility complex I
PD-1	Programmed cell death protein 1
PD-L1	Programmed cell death-ligand 1
dMMR	Mismatch repair deficiency
MSI-H	High microsatellite instability
TCR	T-cell receptor
HLA	Human leukocyte antigen
β2m	β2-Microglobulin
PCSK9	Proprotein convertase subtilisin/kexin type 9
ATCC	American Type Culture Collection
DEGs	Differentially expressed genes
FDR	False discovery rate
GSEA	Gene set enrichment analysis
ANOVA	Analysis of variance
OVA	Ovalbumin
LDH	Lactate dehydrogenase
gDNA	Genomic DNA
GEPIA	Gene expression profiling interactive analysis
COAD	Colon adenocarcinoma
IFN	Interferon

Supplementary Information

The online version contains supplementary material available at https://doi.org/10.1186/s12967-024-05572-2.

Additional file 1: Figure S1. Combined treatment of nilotinib and anti-PDL1 inhibits tumor growth in Balb/c mice. Balb/c mice bearing CT26 xenografts were treated with anti-PDL1 antibody, nilotinibor both. A. Images of tumors from euthanized mice. B. Tumor volume recorded every other day. C. Expression levels of H-2Kd in tumor samples. Results are shown as mean ± SD. *$P<0.05$, ***$P<0.001$, versus control. Figure S2. Neither bosutinib or ponatinib impacts MHC-I expression in HCT116 cells. A. HLA protein expression in HCT116 cells post 24 h bosutinib treatment. B. HLA protein expression in HCT116 post 24 h ponatinib treatment. Results are shown as mean ± SD. ns. $P>0.05$, versus control.

Acknowledgements

We thank Professor Wende Li from Guangdong Laboratory Animals Monitoring Institute for kindly providing OT-I mice.

Author contributions

H.D. designed, performed experiments and wrote original draft; C.W. designed, performed experiments and revised the manuscript; L.H. designed experiments and analyzed the data; J.Z., N.X., L.L. and L.H. performed experiments and analyzed the data; W.L. performed animal experiments; J.L., M.S., Y.H. and S.C. analyzed the data; H.L. and X.Y. designed experiments and revised the manuscript. All authors read and approved the final manuscript.

Funding

This work was supported by National Natural Science Foundation of China (82172337); Guangdong Basic and Applied Basic Research Foundation (2021A1515012530, 2022A1515011316, 2022A1515140001, 2023A1515012377); Guangdong Provincial Clinical Research Center for Digestive Diseases (2020B1111170004); National Key Clinical Discipline.

Availability of data and materials

All the data supporting the findings of this study are available within the paper and its Supplementary Information files. All other data supporting the findings of this study are available from the corresponding author upon reasonable request.

Declarations

Ethics approval and consent to participate

All procedures in animal experiments were conducted following the principles of Animal Research: Reporting of In Vivo Experiments (ARRIVE) 2.0 guidelines and the Basel Declaration. All animal studies were approved by the Committee on the Ethics of Animal Experiments of the Sixth Affiliated Hospital, Sun Yat-sen University (IACUC-2020122502 and IACUC-2021110401). Tissue chip microarray of human colon cancer and adjacent normal tissues (HColA180Su12) was purchased from Shanghai Outdo Biotech Co., Ltd. The study was conducted following the principles of the Declaration of Helsinki and approved by the Ethics Committee of Shanghai Outdo Biotech Co., Ltd. (SHYJS-CP-1607002).

Consent for publication

Not applicable.

Competing interests

The authors declare no competing interests.

Author details

[1]Department of Clinical Laboratory, The Sixth Affiliated Hospital, Sun Yat-Sen University, Guangzhou 510655, Guangdong, China. [2]Guangdong Provincial Key Laboratory of Colorectal and Pelvic Floor Diseases, The Sixth Affiliated Hospital, Sun Yat-Sen University, Guangzhou 510655, Guangdong, China. [3]Department of Obstetrics and Gynecology, The Tenth Affiliated Hospital of Southern Medical University, Dongguan 523059, Guangdong, China. [4]Department of Radiation and Cellular Oncology, University of Chicago, Chicago, IL 60637, USA. [5]Guangdong Institute of Gastroenterology, The Sixth Affiliated Hospital, Sun Yat-Sen University, Guangzhou 510655, Guangdong, China. [6]Department of General Surgery, The Sixth Affiliated Hospital, Sun Yat-Sen University, Guangzhou 510655, Guangdong, China. [7]Biomedical Innovation Center, The Sixth Affiliated Hospital, Sun Yat-Sen University, Guangzhou 510655, Guangdong, China. [8]Department of Neurology, The Sixth Affiliated Hospital, Sun Yat-Sen University, Guangzhou 510655, Guangdong, China. [9]Department of Clinical Laboratory Medicine, the People's Hospital of Guangxi Zhuang Autonomous Region, Nanning 530021, Guangxi, China. [10]Guangdong Laboratory, GuangdongKey Laboratory Animal Lab, Animals Monitoring Institute, Guangzhou 510633, Guangdong, China.

Received: 20 May 2024 Accepted: 4 August 2024
Published online: 14 August 2024

References

1. Ribas A, Wolchok JD. Cancer immunotherapy using checkpoint blockade. Science. 2018;359:1350–5.

2. Fan A, Wang B, Wang X, Nie Y, Fan D, Zhao X, et al. Immunotherapy in colorectal cancer: current achievements and future perspective. Int J Biol Sci. 2021;17:3837–49.
3. Liu B, Song Y, Liu D. Recent development in clinical applications of PD-1 and PD-L1 antibodies for cancer immunotherapy. J Hematol Oncol. 2017;10:174.
4. Overman MJ, McDermott R, Leach JL, Lonardi S, Lenz HJ, Morse MA, et al. Nivolumab in patients with metastatic DNA mismatch repair-deficient or microsatellite instability-high colorectal cancer (CheckMate 142): an open-label, multicentre, phase 2 study. Lancet Oncol. 2017;18:1182–91.
5. Boland CR, Goel A. Microsatellite instability in colorectal cancer. Gastroenterology. 2010;138:2073-2087.e3.
6. Le DT, Kim TW, Van Cutsem E, Geva R, Jäger D, Hara H, et al. Phase II open-label study of pembrolizumab in treatment-refractory, microsatellite instability-high/mismatch repair-deficient metastatic colorectal cancer: KEYNOTE-164. J Clin Oncol. 2020;38:11–9.
7. Chen DS, Mellman I. Oncology meets immunology: the cancer-immunity cycle. Immunity. 2013;39:1–10.
8. Yamamoto K, Venida A, Yano J, Biancur DE, Kakiuchi M, Gupta S, et al. Autophagy promotes immune evasion of pancreatic cancer by degrading MHC-I. Nature. 2020;581:100–5.
9. Fang Y, Wang L, Wan C, Sun Y, Van der Jeught K, Zhou Z, et al. MAL2 drives immune evasion in breast cancer by suppressing tumor antigen presentation. J Clin Invest. 2021;131: e140837.
10. Wieczorek M, Abualrous ET, Sticht J, Álvaro-Benito M, Stolzenberg S, Noé F, et al. Major histocompatibility complex (MHC) class I and MHC class II proteins: conformational plasticity in antigen presentation. Front Immunol. 2017;8:292.
11. Dersh D, Hollý J, Yewdell JW. A few good peptides: MHC class I-based cancer immunosurveillance and immunoevasion. Nat Rev Immunol. 2021;21:116–28.
12. Gu SS, Zhang W, Wang X, Jiang P, Traugh N, Li Z, et al. Therapeutically increasing MHC-I expression potentiates immune checkpoint blockade. Cancer Discov. 2021;11:1524–41.
13. Demel UM, Böger M, Yousefian S, Grunert C, Zhang L, Hotz PW, et al. Activated SUMOylation restricts MHC class I antigen presentation to confer immune evasion in cancer. J Clin Invest. 2022;132: e152383.
14. Burr ML, Sparbier CE, Chan KL, Chan YC, Kersbergen A, Lam EYN, et al. An evolutionarily conserved function of polycomb silences the MHC class I antigen presentation pathway and enables immune evasion in cancer. Cancer Cell. 2019;36(4):385-401.e8.
15. Shklovskaya E, Rizos H. MHC class I deficiency in solid tumors and therapeutic strategies to overcome it. Int J Mol Sci. 2021;22:6741.
16. Luo N, Nixon MJ, Gonzalez-Ericsson PI, Sanchez V, Opalenik SR, Li H, et al. DNA methyltransferase inhibition upregulates MHC-I to potentiate cytotoxic T lymphocyte responses in breast cancer. Nat Commun. 2018;9:248.
17. Wang X, Waschke BC, Woolaver RA, Chen Z, Zhang G, Piscopio AD, et al. Histone deacetylase inhibition sensitizes PD1 blockade-resistant B-cell lymphomas. Cancer Immunol Res. 2019;7:1318–31.
18. Nguyen EM, Taniguchi H, Chan JM, Zhan YA, Chen X, Qiu J, et al. Targeting lysine-specific demethylase 1 rescues major histocompatibility complex class i antigen presentation and overcomes programmed death-ligand 1 blockade resistance in SCLC. J Thorac Oncol. 2022;17:1014–31.
19. Xu H, Van der Jeught K, Zhou Z, Zhang L, Yu T, Sun Y, et al. Atractylenolide I enhances responsiveness to immune checkpoint blockade therapy by activating tumor antigen presentation. J Clin Invest. 2021;131: e146832.
20. Weisberg E, Manley P, Mestan J, Cowan-Jacob S, Ray A, Griffin JD. AMN107 (nilotinib): a novel and selective inhibitor of BCR-ABL. Br J Cancer. 2006;94:1765–9.
21. Giles FJ, Abruzzese E, Rosti G, Kim DW, Bhatia R, Bosly A, et al. Nilotinib is active in chronic and accelerated phase chronic myeloid leukemia following failure of imatinib and dasatinib therapy. Leukemia. 2010;24:1299–301.
22. Archibald M, Pritchard T, Nehoff H, Rosengren RJ, Greish K, Taurin S. A combination of sorafenib and nilotinib reduces the growth of castrate-resistant prostate cancer. Int J Nanomedicine. 2016;11:179–200.
23. Gong W, Yang L, Wang Y, Xian J, Qiu F, Liu L, et al. Analysis of survival-related lncRNA landscape identifies a role for LINC01537 in energy metabolism and lung cancer progression. Int J Mol Sci. 2019;20:3713.
24. Wang F, Hou W, Chitsike L, Xu Y, Bettler C, Perera A, et al. ABL1, overexpressed in hepatocellular carcinomas, regulates expression of NOTCH1 and promotes development of liver tumors in mice. Gastroenterology. 2020;159:289-305.e16.
25. Purcarea A, Jarosch S, Barton J, Grassmann S, Pachmayr L, D'Ippolito E, et al. Signatures of recent activation identify a circulating T cell compartment containing tumor-specific antigen receptors with high avidity. Sci Immunol. 2022;7:eabm2077.
26. Efremova M, Rieder D, Klepsch V, Charoentong P, Finotello F, Hackl H, et al. Targeting immune checkpoints potentiates immunoediting and changes the dynamics of tumor evolution. Nat Commun. 2018;9:32.
27. Zhou Y, Bastian IN, Long MD, Dow M, Li W, Liu T, et al. Activation of NF-κB and p300/CBP potentiates cancer chemoimmunotherapy through induction of MHC-I antigen presentation. Proc Natl Acad Sci USA. 2021;118: e2025840118.
28. Xu MM, Pu Y, Han D, Shi Y, Cao X, Liang H, et al. Dendritic cells but not macrophages sense tumor mitochondrial DNA for cross-priming through signal regulatory protein α signaling. Immunity. 2017;47:363-373.e5.
29. Falahat R, Perez-Villarroel P, Mailloux AW, Zhu G, Pilon-Thomas S, Barber GN, et al. STING signaling in melanoma cells shapes antigenicity and can promote antitumor T-cell activity. Cancer Immunol Res. 2019;7:1837–48.
30. Yum S, Li M, Fang Y, Chen ZJ. TBK1 recruitment to STING activates both IRF3 and NF-κB that mediate immune defense against tumors and viral infections. Proc Natl Acad Sci U S A. 2021;118: e2100225118.
31. Kitajima S, Tani T, Springer BF, Campisi M, Osaki T, Haratani K, et al. MPS1 inhibition primes immunogenicity of KRAS-LKB1 mutant lung cancer. Cancer Cell. 2022;40:1128-1144.e8.
32. Gettinger S, Choi J, Hastings K, Truini A, Datar I, Sowell R, et al. Impaired HLA class I antigen processing and presentation as a mechanism of acquired resistance to immune checkpoint inhibitors in lung cancer. Cancer Discov. 2017;7:1420–35.
33. Cornel AM, Mimpen IL, Nierkens S. MHC class I downregulation in cancer: underlying mechanisms and potential targets for cancer immunotherapy. Cancers. 2020;12:1760.
34. Liu X, Bao X, Hu M, Chang H, Jiao M, Cheng J, et al. Inhibition of PCSK9 potentiates immune checkpoint therapy for cancer. Nature. 2020;588:693–8.
35. Wang R, Liu H, He P, An D, Guo X, Zhang X, et al. Inhibition of PCSK9 enhances the antitumor effect of PD-1 inhibitor in colorectal cancer by promoting the infiltration of CD8+ T cells and the exclusion of Treg cells. Front Immunol. 2022;13: 947756.
36. Liu S, Deng X, Zhang P, Wang X, Fan Y, Zhou S, et al. Blood flow patterns regulate PCSK9 secretion via MyD88-mediated pro-inflammatory cytokines. Cardiovasc Res. 2020;116:1721–32.
37. Abdelwahed KS, Siddique AB, Mohyeldin MM, Qusa MH, Goda AA, Singh SS, et al. Pseurotin A as a novel suppressor of hormone dependent breast cancer progression and recurrence by inhibiting PCSK9 secretion and interaction with LDL receptor. Pharmacol Res. 2020;158: 104847.
38. Alannan M, Fatrouni H, Trézéguet V, Dittrich-Domergue F, Moreau P, Siegfried G, et al. Targeting PCSK9 in liver cancer cells triggers metabolic exhaustion and cell death by ferroptosis. Cells. 2022;12:62.
39. Fang S, Yarmolinsky J, Gill D, Bull CJ, Perks CM, PRACTICAL Consortium, Davey SG, et al. Association between genetically proxied PCSK9 inhibition and prostate cancer risk: a Mendelian randomisation study. PLoS Med. 2023;20:e1003988.
40. Le DT, Durham JN, Smith KN, Wang H, Bartlett BR, Aulakh LK, et al. Mismatch repair deficiency predicts response of solid tumors to PD-1 blockade. Science. 2017;357:409–13.
41. Rosenthal R, Cadieux EL, Salgado R, Bakir MA, Moore DA, Hiley CT, et al. Neoantigen-directed immune escape in lung cancer evolution. Nature. 2019;567:479–85.
42. Garrido F, Aptsiauri N, Doorduijn EM, Garcia Lora AM, van Hall T. The urgent need to recover MHC class I in cancers for effective immunotherapy. Curr Opin Immunol. 2016;39:44–51.
43. Reichardt P, Blay JY, Gelderblom H, Schlemmer M, Demetri GD, Bui-Nguyen B, et al. Phase III study of nilotinib versus best supportive care with or without a TKI in patients with gastrointestinal stromal tumors resistant to or intolerant of imatinib and sunitinib. Ann Oncol. 2012;23:1680–7.
44. Lee SJ, Kim TM, Kim YJ, Jang KT, Lee HJ, Lee SN, et al. Phase II trial of nilotinib in patients with metastatic malignant melanoma harboring KIT

gene aberration: a multicenter trial of Korean cancer study group (UN10-06). Oncologist. 2015;20:1312–9.
45. Jeitany M, Leroy C, Tosti P, Lafitte M, Le Guet J, Simon V, et al. Inhibition of DDR1-BCR signalling by nilotinib as a new therapeutic strategy for metastatic colorectal cancer. EMBO Mol Med. 2018;10: e7918.
46. Shi W, Qiu Q, Feng Z, Tong Z, Guo W, Zou F, et al. Design, synthesis and immunological evaluation of self-assembled antigenic peptides from dual-antigen targets: a broad-spectrum candidate for an effective anti-breast cancer therapy. J Immunother Cancer. 2021;9: e002523.
47. Liu SQ, Grantham A, Landry C, Granda B, Chopra R, Chakravarthy S, et al. A CRISPR screen reveals resistance mechanisms to CD3-bispecific antibody therapy. Cancer Immunol Res. 2021;9:34–49.
48. Ayers M, Lunceford J, Nebozhyn M, Murphy E, Loboda A, Kaufman DR, et al. IFN-γ-related mRNA profile predicts clinical response to PD-1 blockade. J Clin Invest. 2017;127:2930–40.
49. Du W, Hua F, Li X, Zhang J, Li S, Wang W, et al. Loss of optineurin drives cancer immune evasion via palmitoylation-dependent IFNGR1 lysosomal sorting and degradation. Cancer Discov. 2021;11:1826–43.
50. Xiong W, Gao X, Zhang T, Jiang B, Hu MM, Bu X, et al. USP8 inhibition reshapes an inflamed tumor microenvironment that potentiates the immunotherapy. Nat Commun. 2022;13:1700.
51. Forloni M, Albini S, Limongi MZ, Cifaldi L, Boldrini R, Nicotra MR, et al. NF-kappaB, and not MYCN, regulates MHC class I and endoplasmic reticulum aminopeptidases in human neuroblastoma cells. Cancer Res. 2010;70:916–24.
52. Caiazza C, Brusco T, D'Alessio F, D'Agostino M, Avagliano A, Arcucci A, et al. The lack of STING impairs the MHC-I dependent antigen presentation and JAK/STAT signaling in murine macrophages. Int J Mol Sci. 2022;23:14232.
53. Carroll EC, Jin L, Mori A, Muñoz-Wolf N, Oleszycka E, Moran HBT, et al. The vaccine adjuvant chitosan promotes cellular immunity via DNA sensor cGAS-STING-dependent induction of type I interferons. Immunity. 2016;44:597–608.
54. Shen M, Chen C, Guo Q, Wang Q, Liao J, Wang L, et al. Systemic delivery of mPEG-masked trispecific T-cell nanoengagers in synergy with STING agonists overcomes immunotherapy resistance in TNBC and generates a vaccination effect. Adv Sci. 2022;9: e2203523.
55. Deng G, Zhou L, Wang B, Sun X, Zhang Q, Chen H, et al. Targeting cathepsin B by cycloastragenol enhances antitumor immunity of CD8 T cells via inhibiting MHC-I degradation. J Immunother Cancer. 2022;10: e004874.
56. Lin W, Chen L, Zhang H, Qiu X, Huang Q, Wan F, et al. Tumor-intrinsic YTHDF1 drives immune evasion and resistance to immune checkpoint inhibitors via promoting MHC-I degradation. Nat Commun. 2023;14:265.
57. Chen X, Lu Q, Zhou H, Liu J, Nadorp B, Lasry A, et al. A membrane-associated MHC-I inhibitory axis for cancer immune evasion. Cell. 2023;186:3903-3920.e21.
58. Maxwell KN, Fisher EA, Breslow JL. Overexpression of PCSK9 accelerates the degradation of the LDLR in a post-endoplasmic reticulum compartment. Proc Natl Acad Sci U S A. 2005;102:2069–74.
59. Gan ES, Tan HC, Le DHT, Huynh TT, Wills B, Seidah NG, et al. Dengue virus induces PCSK9 expression to alter antiviral responses and disease outcomes. J Clin Invest. 2020;130:5223–34.
60. Wong CC, Wu JL, Ji F, Kang W, Bian X, Chen H, et al. The cholesterol uptake regulator PCSK9 promotes and is a therapeutic target in APC/KRAS-mutant colorectal cancer. Nat Commun. 2022;13:3971.
61. Wu X, Sun L, Xu F. NF-κB in cell deaths, therapeutic resistance and nanotherapy of tumors: recent advances. Pharmaceuticals. 2023;16:783.

Publisher's Note